



Journal of Advanced Research in Fluid Mechanics and Thermal Sciences

Journal homepage:
https://semarakilmu.com.my/journals/index.php/fluid_mechanics_thermal_sciences/index
ISSN: 2289-7879



Analytical Analysis on the Capillary Pressure of Underfill Flow Meniscus During the Flip-Chip Encapsulation Process

Fei Chong Ng¹, Lun Hao Tung¹, Mohamad Aizat Abas^{1,*}

¹ School of Mechanical Engineering, Universiti Sains Malaysia, Engineering Campus, Nibong Tebal, 14300, Penang, Malaysia

ARTICLE INFO

Article history:

Received 10 January 2022
Received in revised form 19 March 2022
Accepted 25 March 2022
Available online 27 April 2022

Keywords:

Bump pitch; electronic packaging;
capillary pressure; contact angle; flip-chip; underfill encapsulation process

ABSTRACT

In the conventional flip-chip underfill encapsulation process, the underfill fluid is driven into the gap beneath the chip and substrate through capillary action. Particularly, the capillary pressure of the flow front determined the strength of overall capillary flow advancement through the bump array, hence the filling time and subsequently the manufacturing productivity. This paper analytically studied the capillary pressure of the flow front. Accordingly, the variation effects of bump contact angle and bump pitch on the flow front capillary pressure were presented. It was found that the variation trend of capillary pressure along the flow displacement between the region confined by two adjacent bumps is sinusoidal. The magnitude of capillary pressure is positive near bump entrant and acting along the flow direction before the capillary pressure gradually decreasing to oppose the flow advancement. The increasing of contact angle shifted the capillary pressure trend leftward with the peak being lowered, whereas the magnitude of capillary pressure decreases with the increases in bump pitch. Additionally, by studying the capillary pressure of flow meniscus, a new dynamic-based contact line jump criterion was proposed by considered the peak capillary pressure along the underfill advancement. These findings are practically useful for the design optimization of flip-chip package to promote the longevity of electronic package and reduce electronic wastes.

1. Introduction

Electronic packaging is the production of interconnection, enclosure and protection that bridging the silicon chip to become the final electronic products. Apart from completing the electronic circuits, the electronics packaging also provides heat dissipation mechanism, mechanical supports, and protective layer against external environment. The electronic packaging aims to promote the reliability, productivity, and longevity of the electronic device [1 – 3].

In the electronic manufacturing and assembly industry, the underfill encapsulation is conducted on the flip-chip package to safeguard the solder joints. It is conducted by dispensing the underfill fluid into the small gap beneath the chip and substrate, as illustrated in Figure 1. The underfill process of flip-chip is regarded as the first hierarchy level of the electronic packaging. The main purpose of

* Corresponding author.

E-mail address: aizatabas@usm.my

underfill process is to address the thermal mismatch issue that caused by the difference the coefficient of thermal expansions (CTE) between the substrate, chip, and solder bump [3 – 5].

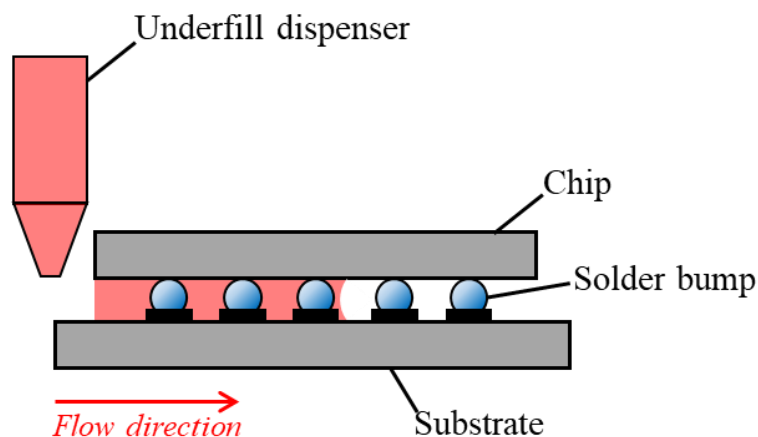


Fig. 1. Underfill dispensing process on a flip-chip package [4]

Conventionally, the flow advancement of underfill fluid during the flip-chip underfill process is solely driven by means of capillarity. Due to the surface tension of meniscus formed at the flow front, the lowered capillary pressure at flow front established a driving pressure gradient with respect to the inlet. Nonetheless, there are various variations of underfill process that adopted external applied force to accelerate the underfill flow, for instance, pressurized, gravity-assisted [1, 2] and thermocapillary [6]. Still the conventional capillary underfill is the most widely used variation in the industry, as has the lowest occurrence of voiding [7, 8].

In the earlier analytical works on underfill process, the capillary pressure of underfill flow front was modelled as constant [9]. Young introduced the mathematical expression of variable capillary pressure of the flow meniscus that subtended between two adjacent solder bumps [10, 11]. The impact and applicability of variable capillary pressure is well demonstrated in the subsequent works on the development of analytical filling time models [12 - 15]. However, for simplicity, the variations of bump capillary pressure were averaged out over each bump. Additionally, the evolution of flow meniscus from concave to convex [16, 17] was closely related to the variation of bump capillary pressure. It was found that both bump pitch and contact angle significantly affected the capillary pressure and thus the capillarity flow and filling time of the underfill process [18, 19].

Generally, the capillary pressure of flow front was scarcely being investigated nor discussed in the underfill research works. To the best knowledge of authors, there is no literature that particularly study the variation effect of underfill parameters on the capillary pressure of underfill flow front as well as the variations of capillary pressure. Therefore, this paper attempts to thoroughly analyze the capillary pressure in the flow meniscus of underfill fluid. Moreover, the variation effects of bump pitch and contact angle on the capillary pressure are presented.

2. Methodology

Capillary pressure of flow meniscus, there are two distinct capillary sources that sustained the flow advancement of the underfill fluid flow through the flip-chip bump array. One of them is the capillary pressure contributed by the parallel surfaces of chip and substrate along the side principle plane as shown in Figure 2; while another component of capillary pressure is contributed by the solder bump surfaces along the side principle plane as shown in Figure 3. Mathematically, in the

region confined by two adjacent bumps, the total magnitude of capillary pressure exerted on the flow meniscus, P_c is simply the additive of both components:

$$P_c = P_{c,c/s} + P_{c,b}, \quad (1)$$

where $P_{c,c/s}$ and $P_{c,b}$ correspond to the capillary pressure terms by the chip-substrate parallel surfaces and the solder bump surfaces respectively.

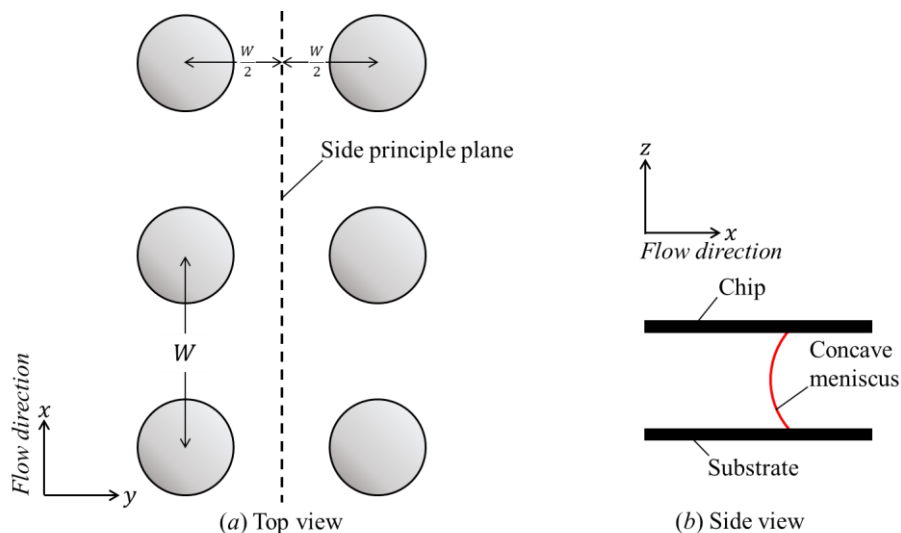


Fig. 2. Flow meniscus along the side principle plane that lies on the x - z plane at mid-bump section

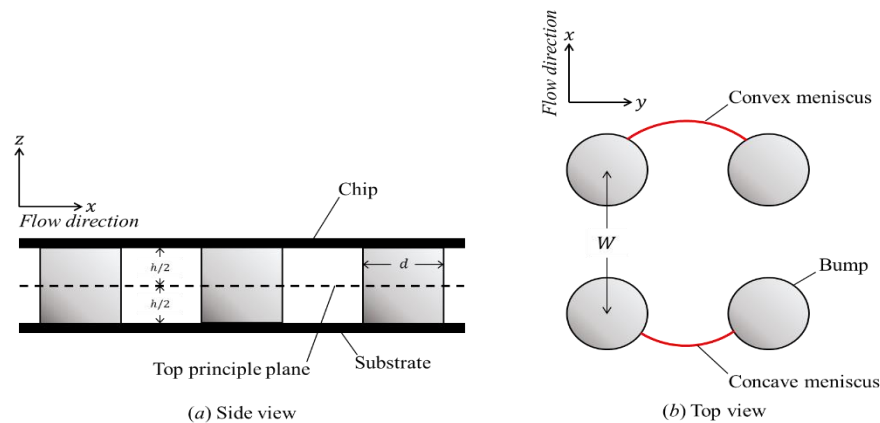


Fig. 3. Flow meniscus along the top principle plane that lies on the x - y plane at level of $z = 0$

Based on the Young-Laplace formulation, the capillary pressure can be expressed in terms of surface tension, σ and contact angle, θ , together with the dimensional parameters as depicted in Figure 4, for instance gap height, h , bump diameter, d and bump pitch, W , as follows

$$P_{c,c/s} = \frac{\sigma}{h} (\cos \theta_c + \cos \theta_s) \quad (2)$$

$$P_{c,b}(\phi) = \frac{2\sigma \cos(\theta_b + \phi)}{W - d \cos \phi} \quad (3)$$

where θ_c , θ_s and θ_b denoted the contact angle of the underfill fluid at the surface of chip, substrate and solder bump respectively [10, 11].

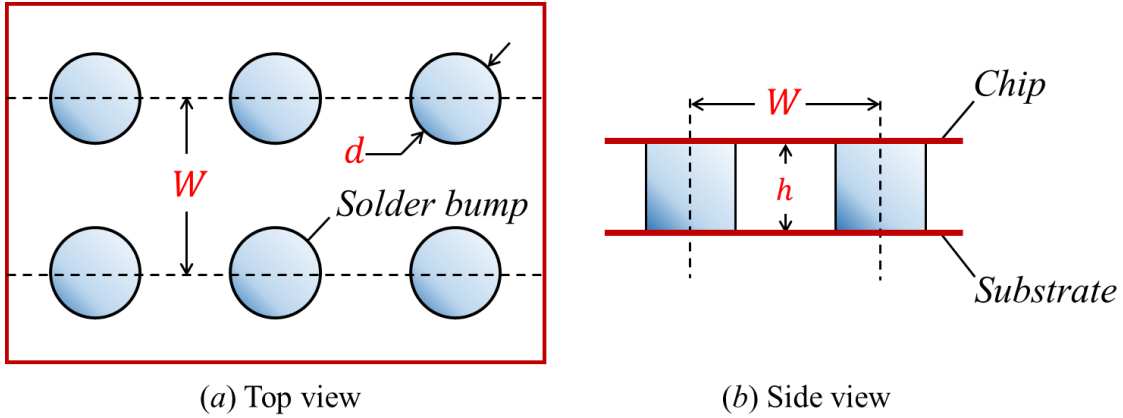


Fig. 4. Geometrical dimensions of a flip-chip bump array [17]

It is noted that the pressure term $P_{c,b}$ is expressed as the function of angular displacement seen from the center of solder bump, ϕ . Therefore, the capillary pressure of underfill flow in the bump confining region is variable and dependent on the instantaneous location of the flow. This is due to the curvature of solder bump surface at the particular flow position. On contrary, the pressure term $P_{c,c/s}$ that arose from both chip and substrate remains constant throughout the underfill flow. As such, the shape of flow meniscus is closely related to the capillary pressure. The meniscus subtended between chip and substrate surface shown in Figure 2(b) is always concave, provided that $\theta_c, \theta_s > \pi/2$. Meanwhile, the meniscus subtended by two adjacent solder bumps given in Figure 3(b) would evolves from concave to convex, when the underfill flow advancing through the bump array.

By introducing the dimensionless bump pitch, W^* , based on the bump diameter, d

$$W^* = \frac{W}{d} \tag{4}$$

and the dimensionless capillary pressure:

$$P_{c,b}^* = \frac{d}{2\sigma} P_{c,b} \tag{5}$$

the equation (3) was non-dimensionalized and thus being reduced to:

$$P_{c,b}^*(\phi) = \frac{\cos(\theta_b + \phi)}{W^* - \cos \phi} \tag{6}$$

The surface tension, σ in Equation (5) can be thought as a constant of proportionality, thus $P_{c,b}^*$ can be thought as a spatial parameter since it only dependent by W^* and θ_b . This is consistent to the fact where the capillary pressure largely dependent on the shape of flow meniscus.

3. Results and discussion

3.1 Validation

Figure 5 compared the proposed analytical formulated underfill flow menisci with the respective experimental [16] and numerical simulated menisci [20] at four filling stages. The concavity of the flow menisci is both the geometrical interpretation and visualization of the capillary strength of underfill flow. It was found that the current proposed analytical model in great consensus with the both the experimental and numerical findings. There is a slight deviation at the bump entrant in which the analytical model predicts concave meniscus with larger convexity. This was attributed to the different dispensing mechanism of underfill fluid in the inlet in analytical formulation. In actual experimental and simulation model, the underfill fluid is continuously dispended at constant rate. Meanwhile, the dispensing rate of underfill fluid is equated to the advancement rate of the flow meniscus.

On the overall trend of meniscus evolution, the shape of flow menisci changes from concave to convex as it advances through the bump array. In bump entrant and during the attach jump (i.e., entrance CLJ), the concave meniscus corresponds to positive bump capillary pressure which assisting the flow advancement. Meanwhile, the convex meniscus with negative bump capillary pressure resisted the flow advancement during exiting the bump array. The lower net driving pressure in the vicinity of bump exit caused the deceleration of underfill flow and giving a longer filling time for the exiting flow and detach jump (i.e., exit CLJ).

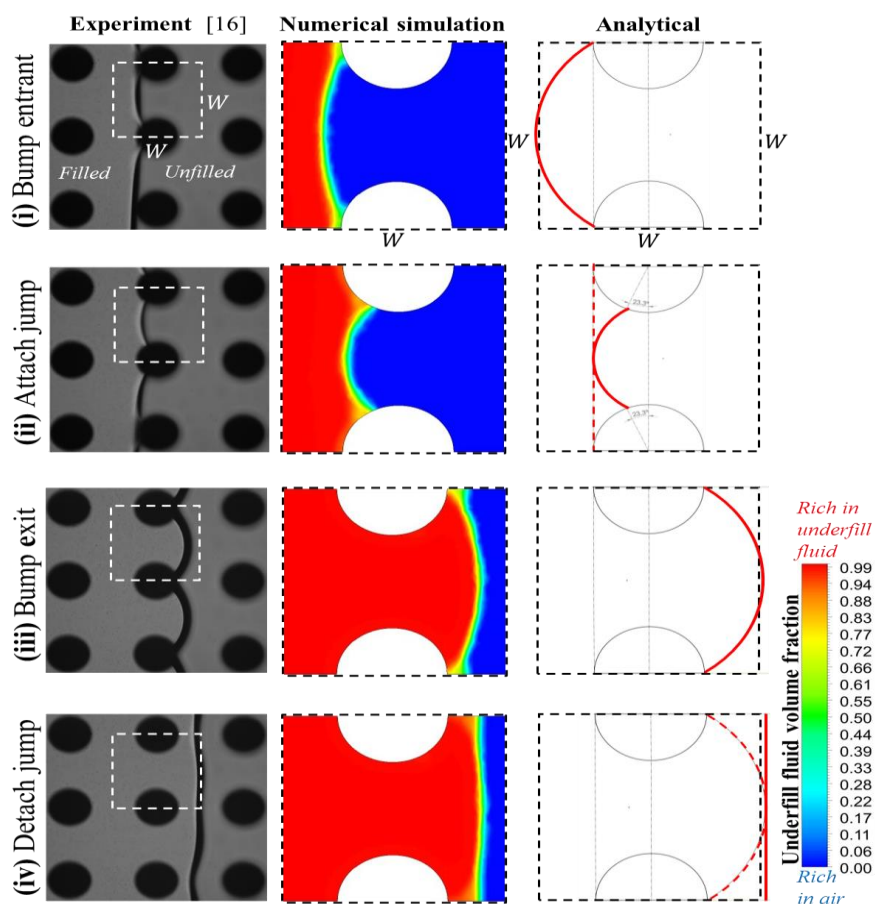


Fig. 5. Comparison of proposed analytical formulated flow menisci with the past underfill experiment [16] and numerical simulation [20]

3.2 Effect of Bump Contact Angle on Capillary Pressure

Figure 6 depicts the variation of bump capillary pressure along the bump region for different values of bump contact angle, θ_b . Initially at the bump entrance, the concave meniscus with positive capillary pressure assist the flow. As the flow travels into the bump array, the capillary pressure rapidly increasing in magnitude as the bump clearance became narrow until it reaches a peak. The pressure peak occurs earlier than $\phi = 0^\circ$ for the narrowest bump clearance due to the direction of surface force vector which no longer favors the flow direction. Subsequently, the capillary pressure gradually declines in value as the bump clearance become wider as it approaches the bump exit; until become zero at ϕ_c where the meniscus become straight. After the transition point of ϕ_c , the bump switches its role from assisting to resisting, where the convex meniscus of negative capillary pressure is formed. The negative capillary pressure has the largest magnitude at the apex of bump exit, which directly influenced the rate of expansion flow during exit contact line jump (CLJ). On the trend of θ_b , it is found that the peak of capillary pressure becomes lower and shifts to the left with the increasing θ_b . Near the bump exit, the bump capillary pressure increases with the decreasing θ_b . Again, it is affirmed that the low θ_b which implies high wettability of bump surface promotes the flow through bump by giving higher ϕ_c of less formation for the convex meniscus.

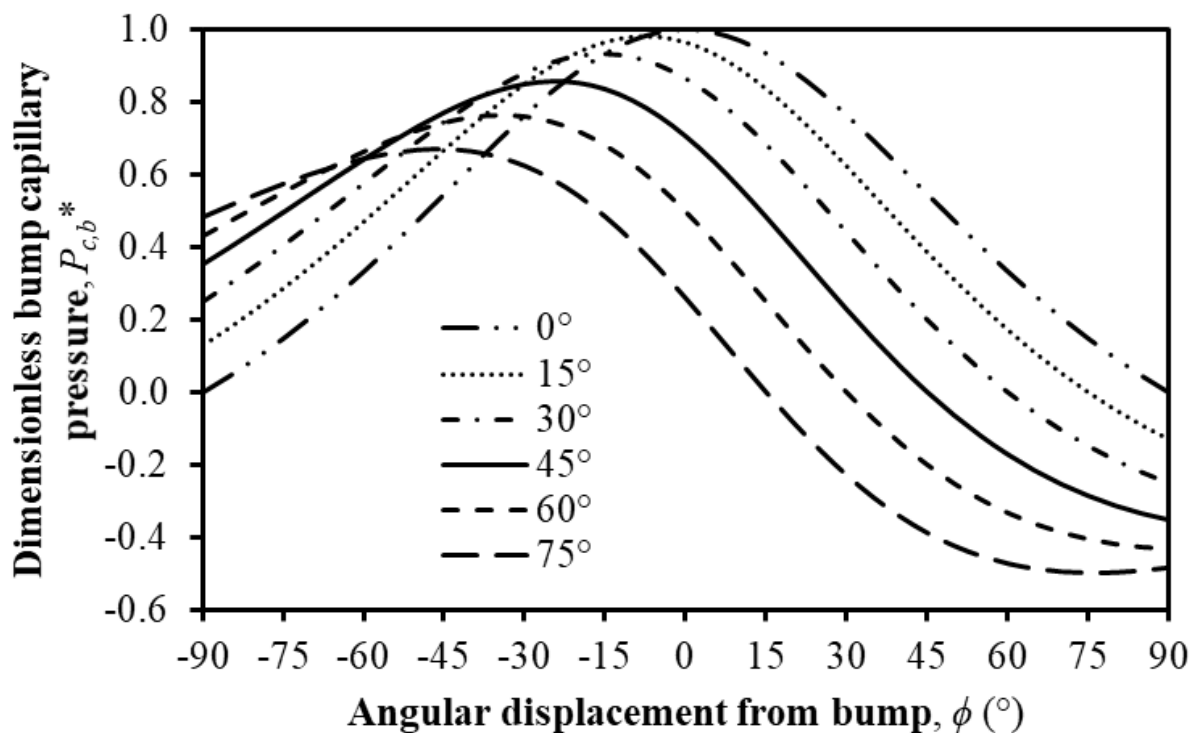


Fig. 6. Plot of $P_{c,b}^*$ against ϕ for various θ_b at fixed $W^* = 2$

3.3 Effect of Bump Pitch on Capillary Pressure

Figure 7 and Figure 8 present the variation of bump capillary pressure for different pitches, respectively at fixed $\theta_b = 0^\circ$ (perfect wetting) and $\theta_b = 60^\circ$ (partial wetting). From Figure 7, it is easily seen that the magnitude of capillary pressure increases as the bump gets shorter. From Figure 8, despite the short bump pitch can increase the assisting capillary pressure of the concave meniscus, the subsequent resisting capillary pressure of convex meniscus is also being enhanced proportionally. Additionally, another less obvious trend is such that the pressure peak tends to shift leftward. Unless the fluid is of very low θ_b to minimize the occurrence of convex meniscus, the short bump pitch is regarded as beneficial in promoting the meniscus advancement.

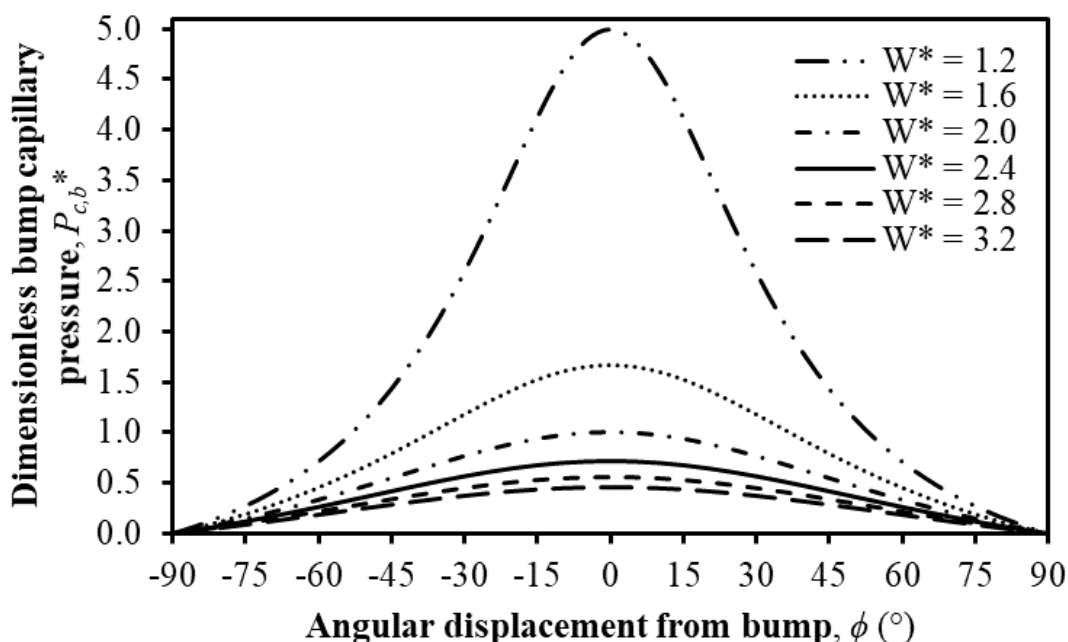


Fig. 7. Plot of $P_{c,b}^*$ against ϕ for various W^* at fixed $\theta_b = 0^\circ$

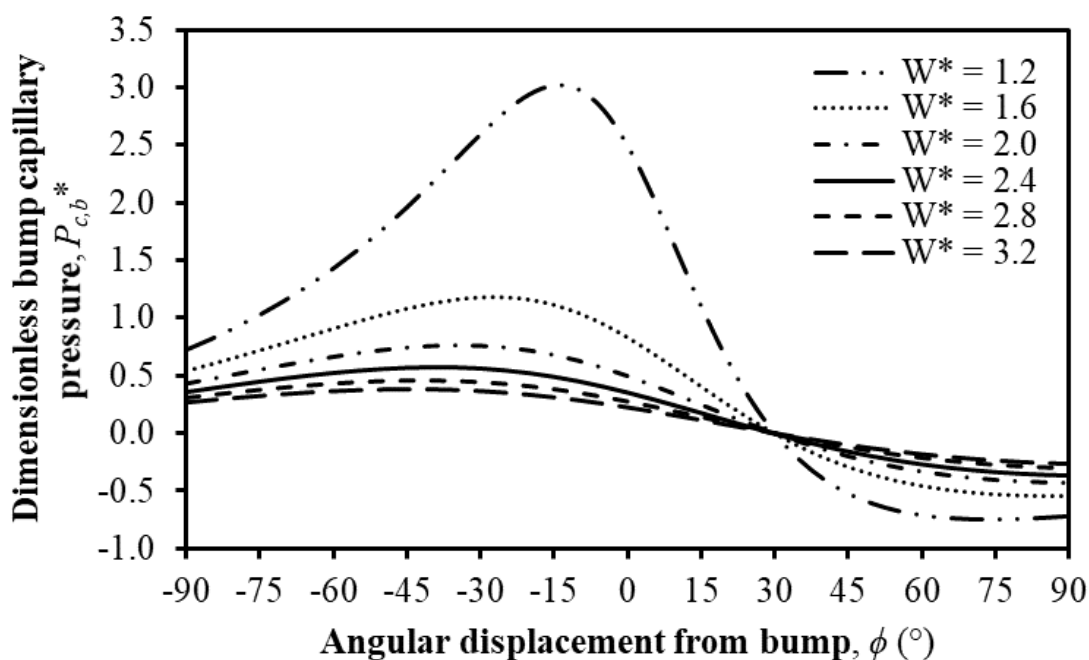


Fig. 8. Plot of $P_{c,b}^*$ against ϕ for various W^* at fixed $\theta_b = 60^\circ$

3.4 Maximal Capillary Pressure at The Entrance Contact Line Jump (CLJ)

Contact line jump (CLJ) is the instantaneous advancement of flow meniscus when it just touched or come close to the solder bump, which occurred at both the entrance and exit of bump arrays. For the entrance CLJ, the pressure difference across the meniscus is high during the jump, leading to an instantaneous CLJ occurrence [10, 11]. By assuming no flow during the occurrence of CLJ, Yao *et al.*, had formulated the angle criterion based on mass conservation when the jump attached to the solder bump [21]. However, such assumption appears to be crude as the underfill fluid being continuously dispensed through the encapsulation process. Accordingly, Ng *et al.*, proposed a new criterion based on minimal flow, in which the center-line displacement is negligible during the jump, but there is fluid advancement in elsewhere [20]. These two CLJ criteria shared the common aspects as they were derived geometrically. This work proposed a new CLJ criterion based on the dynamic aspect of maximal capillary pressure. The motivation behind the formulation of this new criterion is based on Young's discovery and explanation on the CLJ phenomenon where indefinite high pressure is associated to the meniscus during the jump. Generally, the capillary pressure of flow front is contributed by both the chip-substrate (in principle plane 1) and solder bumps array (in principle plane 2). The capillary pressure contributed by chip-substrate pair is constant, $2\sigma \cos \theta_c / h$, evident by fixed concave meniscus; whereas the capillary pressure contributed by the bump varies due to its varying separation and curved geometry. The capillary pressure of flow front due to solder bump array is given as

$$\Delta P_b^* = \frac{\Delta P_b}{2\sigma/W} = \frac{\cos(\theta_b + \phi)}{1 - \cos \phi / W^*} \quad (7)$$

The value of ϕ corresponding to the maximal value of ΔP_b can be found by taking first derivative on equation (7). The entrant jump angle, ξ associated to the maximal capillary pressure CLJ criterion can be solved from the following equation

$$\sin(\theta_b + \xi) (\alpha \cos \xi - 1) - \alpha \cos(\theta_b + \xi) \sin \xi = 0 \quad (8)$$

where the bump density, $\alpha = \frac{d}{W} = \frac{1}{W^*}$.

Figure 9 compared the proposed maximal capillary pressure CLJ criterion with the existing geometrical CLJ criteria. It was found that the proposed dynamic-based CLJ criterion depicted an increasing trend with the bump density, which is opposing with the trends exhibited by geometrical-based CLJ criteria. This is due to different approach taken in formulating the CLJ criteria, in which the current proposed criterion considered the flow dynamics and energetic approach, which did not be considered in the past geometrical criteria.

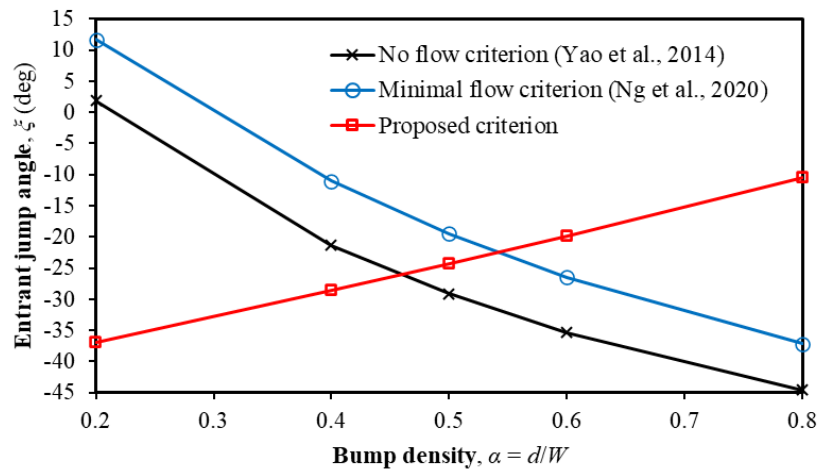


Fig. 9. Comparisons of entrant jump angles proposed from both the past geometrical CLJ criterions [20, 21] and the current dynamic CLJ criterion

4. Conclusions

In this paper, the variation effects of the design parameters of flip-chip and underfill fluid, namely bump pitch and contact angle on the capillary pressure of flow meniscus were studied analytically. The capillary pressure component that contributed by the solder bumps is non-linear and varies sinusoidally along the instantaneous position of flow meniscus, whereas the pressure component due to the parallel surface of chip-substrate pair is constant throughout the flow. Further analysis revealed that the sinusoidal trend of bump contributed capillary pressure is affected by both bump pitch and contact angle. As the bump contact angle increases, the peak of capillary pressure is lowered and the transition point of zero-pressure that determined the meniscus shape shifted leftward. The overall magnitude of capillary pressure decreases with the increases in bump pitch, but the transition point remains invariant with the bump pitch. It is inferred that both the bump pitch and the contact angle of underfill fluid played crucial roles in the underfill packaging process. The underfill fluid of low contact angle and package with dense bump array are desired to achieve fast underfill flow and complete filling. Additionally, a new dynamic-based contact line jump criterion was formulated based on the maximal capillary pressure. Nonetheless, the trend of proposed dynamic-based criterion is increasing with the bump density, which is the opposing trend predicted by the past geometrical-based criterions. These findings essentially useful for the design optimization works to enhance the package's reliability and process's performance. As results, the lifespan of the electronic device would be prolonged and thus reduced the electronic wastes to ensure environmental sustainability.

Acknowledgement

The authors would like to gratefully acknowledge the USM Fellowship Award, provided by Institute of Postgraduate Studies (IPS), University Sains Malaysia (USM).

References

- [1] Zhang, Zhuqing, and C. P. Wong. "Recent advances in flip-chip underfill: materials, process, and reliability." *IEEE transactions on advanced packaging* 27, no. 3 (2004): 515-524. <https://doi.org/10.1109/TADVP.2004.831870>
- [2] Ardebili, H. and Pecht, M.G. "Chapter 3 – Encapsulation process technology." *Elsevier, Encapsulation Technologies for Electronic Applications* (2009), 129 – 179. <https://doi.org/10.1016/j.ijfoodmicro.2006.07.008>
- [3] Ng, Fei Chong, and Mohamad Aizat Abas. "Underfill flow in flip-chip encapsulation process: a review." *Journal of Electronic Packaging* 144, no. 1 (2022). <https://doi.org/10.1115/1.4050697>
- [4] Ng, Fei Chong, Aizat Abas, Z. L. Gan, Mohd Zulkifly Abdullah, F. Che Ani, and M. Yusuf Tura Ali. "Discrete phase method study of ball grid array underfill process using nano-silica filler-reinforced composite-encapsulant with varying filler loadings." *Microelectronics Reliability* 72 (2017): 45-64. <https://doi.org/10.1016/j.microrel.2017.03.034>
- [5] Ng, Fei Chong, Aizat Abas, and Mohd Zulkifly Abdullah. "Effect of solder bump shapes on underfill flow in flip-chip encapsulation using analytical, numerical and PIV experimental approaches." *Microelectronics Reliability* 81 (2018): 41-63. <https://doi.org/10.1016/j.microrel.2017.12.025>
- [6] Ng, Fei Chong, Aizat Abas, Muhammad Hafifi Hafiz Ishak, Mohd Zulkifly Abdullah, and Abdul Aziz. "Effect of thermocapillary action in the underfill encapsulation of multi-stack ball grid array." *Microelectronics Reliability* 66 (2016): 143-160. <https://doi.org/10.1016/j.microrel.2016.10.001>
- [7] Abas, Aizat, Fei Chong Ng, Z. L. Gan, M. H. H. Ishak, M. Z. Abdullah, and Gean Yuen Chong. "Effect of scale size, orientation type and dispensing method on void formation in the CUF encapsulation of BGA." *Sādhanā* 43, no. 4 (2018): 1-14. <https://doi.org/10.1007/s12046-018-0849-3>
- [8] Ng, F.C., Abas, A., Abdullah, M.Z., Ishak, M.H.H. and Chong, G.Y. "CUF scaling effect on contact angle and threshold pressure.", *Soldering & Surface Mount Technology* 29 no.4 (2017): 173–190. <https://doi.org/10.1088/1757-899X/203/1/012013>
- [9] Wan, J.W., Zhang, W.J. and Bergstrom, D.J. "An Analytical Model for Predicting the Underfill Flow Characteristics in Flip-Chip Encapsulation." *IEEE Transactions on Advanced Packaging* 28 no.3 (2005): 481 – 487. <https://doi.org/10.1109/TADVP.2005.848385>
- [10] Young, W-B. "Anisotropic behavior of the capillary action in flip chip underfill." *Microelectronics Journal* 34 (2003): 1031 – 1036. <https://doi.org/10.1016/j.mejo.2003.09.001>
- [11] Young, W-B. "Capillary impregnation into cylinder banks." *Journal of Colloid and Interface Science* 273 (2004): 576 – 580. <https://doi.org/10.1016/j.jcis.2003.11.056>
- [12] Ng, F.C., Abas, A. and Abdullah, M.Z. "Regional segregation with spatial considerations based analytical filling time model for non-Newtonian power-law underfill fluid in flip-chip encapsulation." *Journal of Electronic Packaging* (2019), 141(4): 041009. <https://doi.org/10.1115/1.4044817>
- [13] Ng, F.C., Abas, A. and Abdullah, M.Z. "Filling efficiency of flip-chip underfill encapsulation process." *Soldering & Surface Mount Technology* (2019), 32 no. 1 :10–18. <https://doi.org/10.1108/SSMT-07-2019-0026>
- [14] Ng, F.C., Tura Ali, M.Y., Abas, A., Khor, C. Y., Samsudin, Z. and Abdullah, M. Z. "A novel analytical filling time chart for design optimization of flip-chip underfill encapsulation process." *The International Journal of Advanced Manufacturing Technology* (2019). 105:3521–3530. <https://doi.org/10.1007/s00170-019-04573-6>
- [15] Ng, F. C. and Abas, M. A., "Surface energetic-based analytical filling time model for flip-chip underfill process." *Soldering & Surface Mount Technology* (2021). <https://doi.org/10.1108/SSMT-10-2020-0042>
- [16] Lee, S.H., Sung, J. and Kim, S.E. "Dynamic flow measurement of capillary underfill through a bump array in flip chip package." *Microelectronics Reliability* 50 (2010): 2078–2083. <https://doi.org/10.1016/j.microrel.2010.07.001>
- [17] Ng, F.C., Abas, A. and Abdullah, M.Z. "Finite volume method study on contact line jump phenomena and dynamic contact angle of underfill flow in flip-chip of various bump pitches." *IOP Conference Series: Materials Science and Engineering* 530, no.1 (2019): 012012. <https://doi.org/10.1088/1757-899X/530/1/012012>
- [18] Ng, Fei Chong, Mohd Hafiz Zawawi, Lun Hao Tung, Mohamad Aizat Abas, and Mohd Zulkifly Abdullah. "Symmetrical unit-cell numerical approach for flip-chip underfill flow simulation." *CFD Letters* 12, no. 8 (2020): 55-63. <https://doi.org/10.37934/cfdl.12.8.5563>
- [19] Ng, Fei Chong, Lun Hao Tung, Mohd Hafiz Zawawi, Muhamed Abdul Fatah Muhamed Mukhtar, Mohamad Aizat Abas, and Mohd Zulkifly Abdullah. "Effect of contact angle on meniscus evolution and contact line jump of underfill fluid flow in flip-chip encapsulation." *CFD Letters* 12, no. 6 (2020): 28-38. <https://doi.org/10.37934/cfdl.12.6.2838>
- [20] Ng, Fei Chong, Mohd Hafiz Zawawi, and Mohamad Aizat Abas. "Spatial analysis of underfill flow in flip-chip encapsulation." *Soldering & Surface Mount Technology* (2020). <https://doi.org/10.1108/SSMT-05-2020-0017>
- [21] Yao, X.J., Wang, Z.D. and Zhang, W.J. "A New Analysis of the Capillary Driving Pressure for Underfill Flow in Flip-Chip Packaging." *IEEE Transactions on Components, Packaging and Manufacturing Technology* 4 no.9 (2104): 1534 – 1544. <https://doi.org/10.1109/TCPMT.2014.2339493>